THE CHARACTERISTICS OF ATMOSPHERIC TURBULENCE AS RELATED TO WIND LOADS ON TALL STRUCTURES

George H. Fichtl,[1] John W. Kaufman,[2] and William W. Vaughan[3]

Aerospace Environment Division
Aero–Astrodynamics Laboratory
NASA—Marshall Space Flight Center
Huntsville, Alabama 35812

An engineering boundary layer wind model based upon data collected at the NASA 150-meter meteorological tower facility at the Kennedy Space Center, Florida is discussed. A statistical power-law peak wind profile is used to extrapolate peak wind statistics valid at the 10-meter level to other levels. The relationship between the instantaneous extreme wind profile and the peak wind profile for various periods of exposure up to ten minutes is examined. The gust factor profile, which depends on the peak wind speed, height, and averaging time, is applied to the peak wind profile to obtain a mean wind profile. A spectral model of the longitudinal and lateral components of turbulence for the neutral boundary layer (high wind speeds) is presented.

Key words: Atmospheric boundary layer; gust factors; peak values, power spectra; turbulence; wind profiles.

Nomenclature

b = parameter that characterizes the statistics of k
C_p = specific heat of dry air at constant pressure
C = empirically determined parameter that occurs in formulae of the longitudinal and lateral spectra
f = $nz/\bar{u}$
f_m = value of f associated with peak of logarithmic spectrum
g = acceleration of gravity
g_0 = empirical function of u_{18} and t that occurs in the formula for the gust factor
G = gust factor
k = peak wind profile parameter
k_1 = 0.4 = von Karman's constant
L' = stability length
n = frequency, Hz
p = empirical function of u_{18} that occurs in the formula for the gust factor
r = empirically determined parameter that occurs in formulae of the longitudinal and lateral spectra
Ri = gradient Richardson number
$S(n)$ = longitudinal or lateral spectrum of turbulence
$S_2(n)$ = spectrum of the square of the longitudinal or lateral components of the wind
t = averaging time
$\bar{T}$ = time average mean temperature
$u(z)$ = peak wind speed at height z
$\bar{u}(z)$ = time averaged mean wind speed at height z
u_* = surface friction velocity
z_0 = surface roughness length
β = vertical collapsing factor
σ = variance of k or variance of the longitudinal or lateral components of turbulence
ψ = logarithmic wind profile stability defect.

1. Introduction

The purpose of environmental wind criteria is to provide a model of the atmospheric boundary layer such that when it is used in design studies an acceptable structure results. How one should develop such a model is determined by the purpose and requirements of the structure. Thus, to develop these models so that they are meaningful from an engineering viewpoint, it is necessary that the atmospheric scientist and the design engineer work as a team.

The National Aeronautics and Space Administration, Marshall Space Flight Center (MSFC), Huntsville, Alabama, is concerned with developing and operating launch vehicles like the Saturn V, which placed three American astronauts into lunar orbit on December 25, 1968. The Saturn V stands 363 feet tall and weighs over 6 million pounds. Its height makes the vehicle especially vulnerable to ground wind loads. An artist's concept of this

[1] Aerospace Engineer.
[2] Chief, Atmospheric Dynamics Branch.
[3] Chief, Aerospace Environment Division.

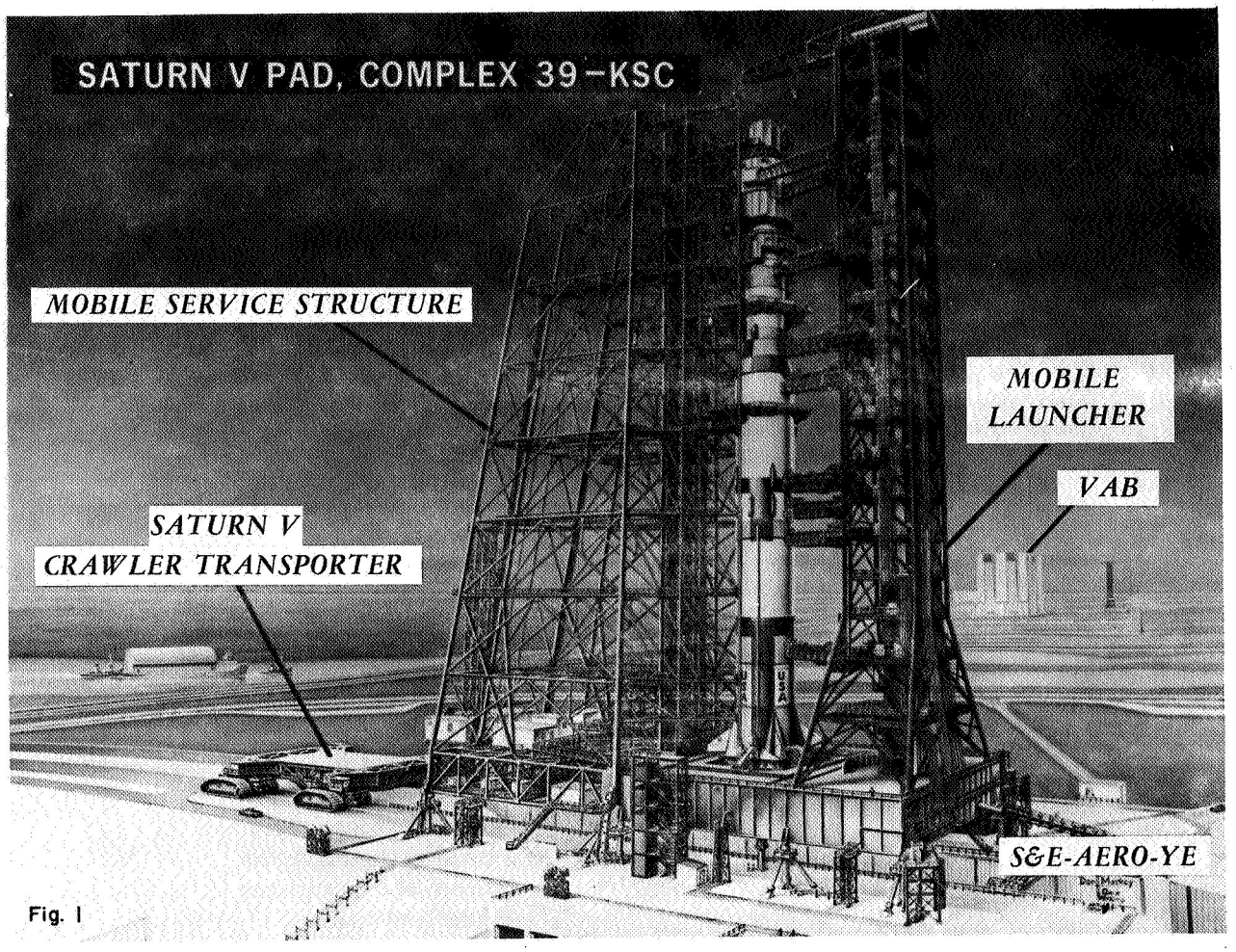

FIGURE 1. An artist's concept of the Saturn V space vehicle and the associated ground support equipment.

vehicle and its associated ground support equipment is shown in Figure 1. About 2 months before launch, the vehicle is erected in the Vertical Assembly Building (see background of Figure 1) on the Mobile Launcher. The vehicle and launcher are then moved to the launch pad, about 3 miles away, on the Crawler Transporter. The Mobile Service Structure is then moved to the vehicle to provide a platform from which the vehicle can be serviced. Before launch, the Mobile Service Structure is rolled off the pad, and the vehicle is launched from the Mobile Launcher.

During the design and fabrication stages of space vehicles, the design engineer must know the final weight of the launch configuration so that unnecessary weight penalties are avoided. Since the ground support equipment will remain on the ground at launch, the present design philosophy in the industry is to design the auxiliary ground support equipment to alleviate, wherever practical, some of the loads on the vehicle due to the ground winds. However, it is conceivable that ground support equipment may have to be so sophisticated that providing this capability will become impractical. Thus, it is imperative that the ground wind environment be defined in usable engineering terms as precisely as possible so that the engineer need not overdesign the ground support equipment and the vehicle structure for a given value of risk. This is especially true if the vehicle is required to withstand ground wind loads in the event the ground support equipment cannot be designed to completely alleviate the entire design ground wind loadings. Although there are various ways of presenting wind criteria for engineering design, this paper describes only the principal methods used at the Marshall Space Flight Center.

2. Peak Wind Statistics

The fundamental surface wind statistics for the Kennedy Space Center are based on an 8-year sample of hourly peak wind speeds measured at the 10-meter level for a period of record from September 1958 through June 1967. The sample was constructed for NASA at the National Weather Records Center, Asheville, North Carolina, by selecting the peak wind speed that occurred in each hour of record read from original wind rolls. Peak wind statistics have three advantages over mean wind statistics. First, peak wind statistics do not depend on an averaging operation as do mean wind statistics. Second, to construct a sample of mean winds, a chart reader or weather observer must perform an "eye-ball" average of the wind data, thus, causing the averaging process to vary from day to day according to the mood of the observer and from observer to observer. Hourly peak wind speed readings avoid this subjective averaging process because "a peak is a peak is a peak." Third, to monitor winds during the countdown phase of a vehicle launch, it is easier and more objective to monitor the peak wind speed than the mean wind speed.

Smith et al. [1]* have performed extensive statistical analyses with the Kennedy Space Center peak wind speed sample. In the course of his work at the Marshall Space Flight Center, he has introduced the concept of exposure period probabilities into the design and operation of space vehicles. By determining the distribution functions of peak wind speeds for various periods of exposure (hour, day, month, year, etc.), it is possible to determine the probability that a certain peak wind-speed magnitude will occur during a prescribed period of exposure of a space vehicle to the natural environment. Thus, for example, if an operation requires, say, one hour to complete, and if the critical wind loads on the vehicle can be defined in terms of the peak wind speed, then it is the probability of occurrence of the peak wind speed during a 1-hour period that gives a measure of the probable risk of the occurrence of structural failure. Similarly, if an operation requires one day to complete, then it is the probability of occurrence of the peak wind during a 1-day period that gives a measure of the probable risk of structural failure.

Smith et al. [1] have also shown that the peak wind speeds at Cape Kennedy for various periods of exposure have a Fisher–Tippett Type I distribution [2], which is the one used by Gumbel [3]. Although the Gumbel distribution appears to give a good theoretical fit to the empirical peak wind speed distribution, it has the disadvantage that it is unbounded at both ends. Since wind speed has a physical lower bound at zero, it may be desirable to investigate other distribution functions. Smith points out that the Fisher-Tippett Type II distribution, which is indeed bounded from below at zero, would be such a function. Thom [4] has used the Fisher-Tippett Type II distribution for representing ground wind statistics.

Figure 2 shows an example of Smith's peak wind speed statistics where the distributions for the month of October for different reference periods are illustrated, and the probabilities of the occurrences of peak wind speeds for the indicated reference periods can be determined. Thus, for example, the probability that the peak wind speed during the hour from 0530 to 0630 EST will be less than 32 knots is 0.977

Probability statements concerning the capabilities of the space vehicles developed at MSFC and launched at the Kennedy Space Center (KSC) are given in terms of Smith's peak wind speed exposure statistics. The statistics are valid at the 10-meter level. However, to perform loading and response calculations resulting from steady-state and random turbulent drag loads and von Karman vortex shedding loads, the engineer requires information about the vertical variation of the mean wind speed and the structure of turbulence in the atmospheric boundary layer. The philosophy at MSFC is to extrapolate the peak wind statistics up into the

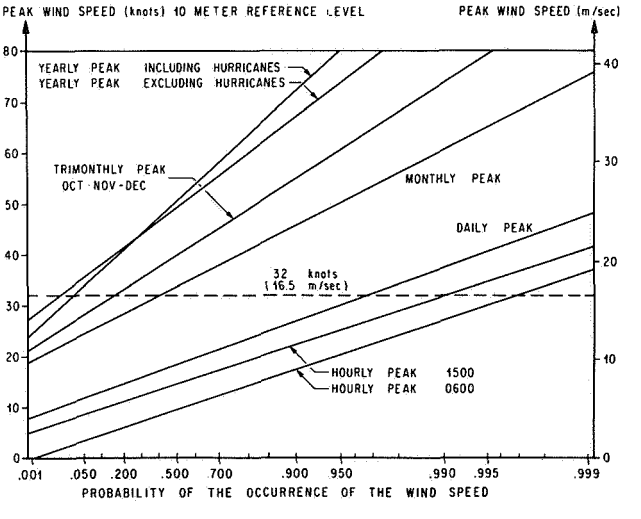

FIGURE 2. Fisher-Tippett distribution collated to peak wind speed samples at Cape Kennedy, Florida, in October.

* Figures in brackets indicate literature references at the end of this paper.

atmosphere using a peak wind profile, and to obtain the associated quasi-steady or mean wind speed profile by applying a gust factor, which is a function of wind speed and height. At this point, the engineer can calculate the steady-state loads resulting from the mean wind profile and the response due to discrete gusts in the form of a gust factor. The gust factor accounts for the loads beyond those resulting from the quasi-steady wind profile—in short, the turbulence. For some applications, depending on the response characteristics of the vehicle, the peak wind speed profile is used directly in the calculations. An alternative, and probably more meaningful, representation of the turbulence can be given in the form of a spectral model of the longitudinal and lateral components of turbulence.

3. The NASA 150-Meter Meteorological Tower

To obtain micrometeorological data representative of the Cape Kennedy area, especially in the vicinity of the Apollo/Saturn V launch pads, a 150-meter meteorological tower was constructed on Merritt Island at the Kennedy Space Center. The tower facility, discussed in detail in a report by Kaufman and Keene [5], is only briefly described here.

3.1. Terrain Features

Figure 3 shows the location of the facility with respect to the Saturn V space vehicle launch complex 39. Located about 3 miles from the Atlantic Ocean, the tower is situated in a well-exposed area free of near-by structures which could interfere with the air flow.

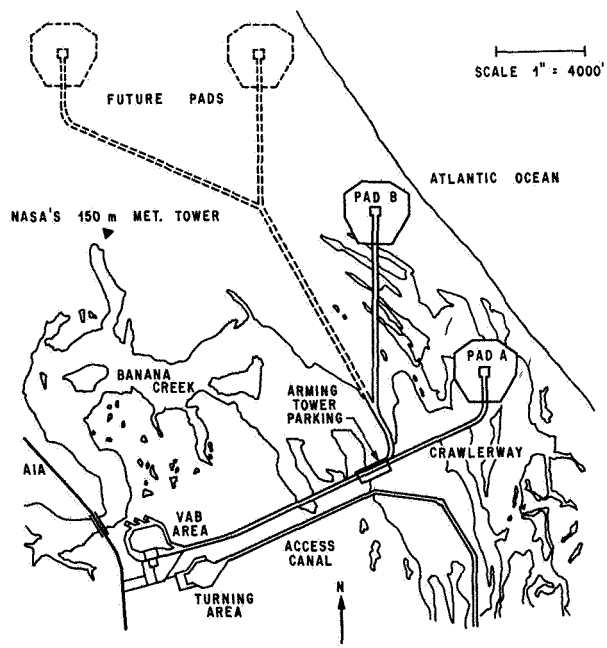

FIGURE 3. NASA Launch Complex 39, Kennedy Space Center, Florida.

The aerial photograph (Fig. 4) of the terrain surrounding the tower (point T) was taken at 3,500 ft above mean sea level. In the quadrant from approximately 300° north azimuth with respect to the tower, clockwise around to 90°, the terrain is homogeneous and is covered with vegetation about ½ to 1½ meters high. Another homogeneous fetch with the same type of vegetation occurs in the 135° to 160° quadrant. The areas A (230° to 300°), B (90° to 135°), and C (160° to 180°) are covered with trees from about 10 to 15 meters tall. The fetch from the tower to areas A or C is about 200 meters, and the fetch to area B is about 450 meters. The height of the vegetation over these fetches ranges from ½ to 1½ meters, as in the area to the north of the tower. To the south–southwest in the 180° to 230° quadrant 225 meters from the tower, there is a body of water called Happy Creek.

3.2. Instrumentation

The complete tower facility comprises two towers, one 18 meters and the other 150 meters high (see Fig. 5). The levels on both towers are instrumented with Climet (Model CI–14) wind sensors. Temperature sensors, Climet (Model–016) aspirated thermocouples, are located at the 3- and 18-meter levels on the small tower and at the 30-, 60-, 120-, and 150-meter levels on the large tower. Foxboro (Model F–2711AG) dewpoint temperature sensors are located at the 60- and 150-meter levels on the large tower and at the 3-meter level on the 18-meter tower. Wind speed and direction data can be recorded on both paper strip charts and analog magnetic tapes with an Ampex FR–1200 fourteen-channel magnetic tape recorder which uses a 14-in reel. The temperature and dewpoint data are recorded on paper strip charts. To avoid tower interference of the flow, the large tower is instrumented with two banks of wind sensors. The details of how and when one switches from one bank of instrumentation to the other bank is discussed by Kaufman and Keene in Reference 5. During a test in which the wind data are stored on magnetic tape, only one bank of instrumentation is used. This avoids interruption of the wind data signals within any magnetic tape recording period, and thus avoids data-processing difficulties when converting analog tapes to digital tapes.

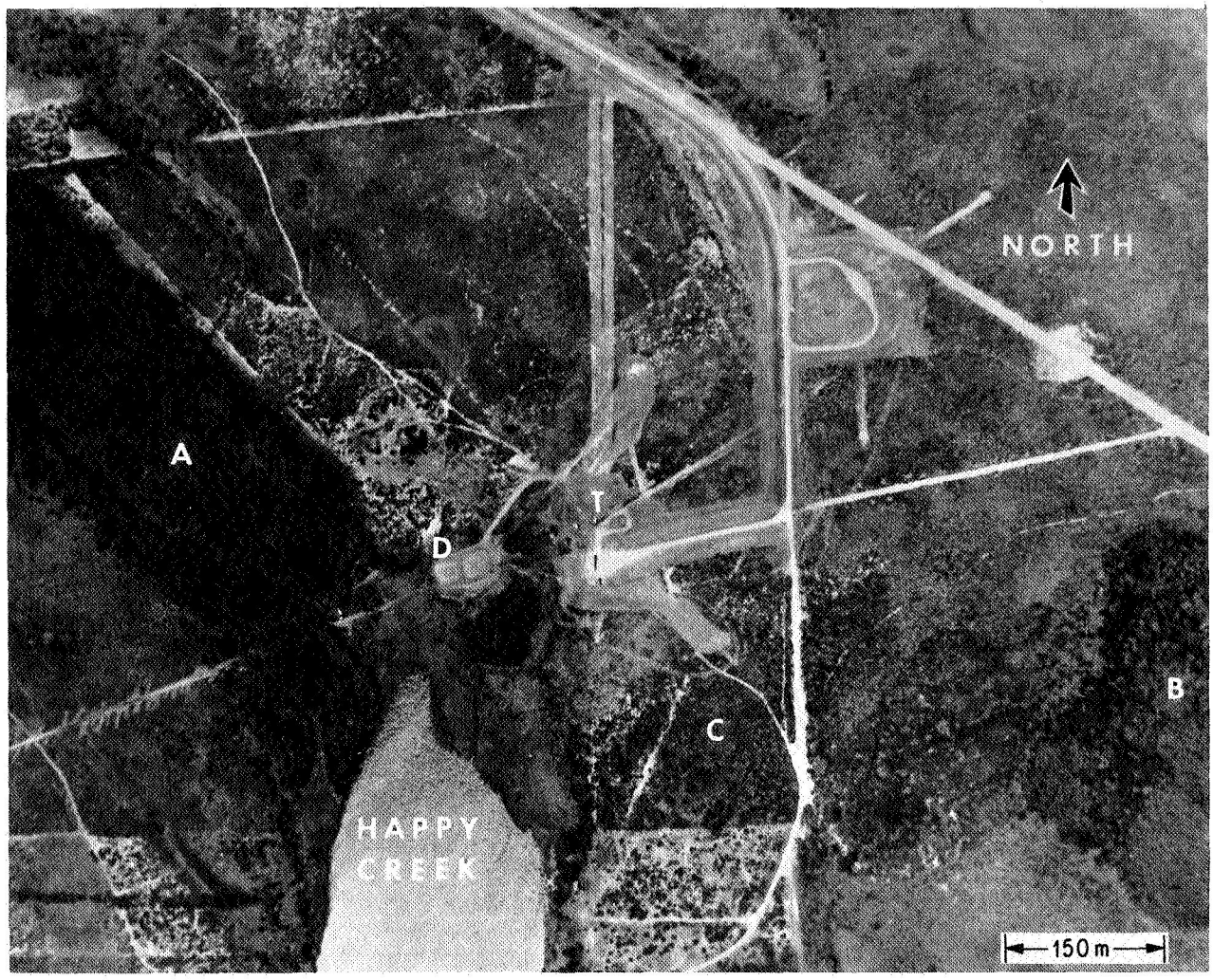

FIGURE 4. Aerial plan view of the terrain surrounding the NASA 150-meter meteorological tower.

3.3. Surface Roughness Length (z_0)

In an earlier report, Fichtl [6] discussed the surface roughness length configuration associated with the NASA meteorological tower. This analysis was based upon wind profile laws that are consistent with the Monin–Obukhov similarity hypothesis. The calculations of z_0 were based on wind data obtained at the 18- and 30-meter levels and on temperature data obtained at the 18- and 60-meter levels. Most of the measurements were obtained during the hours of 0700 and 1600 EST, and the gradient Richardson numbers at 23 meters (geometric height between 18 and 30 meters) for the 39 cases ranged between -5.82 and $+0.079$. The results of these calculations, shown in Figure 6, show the effect the terrain features (see Section IIIa) have upon the surface roughness.

4. Design Wind Profiles

To calculate wind loads on space vehicles, the engineer requires specific information about the wind profile. As pointed out in Section II, the fundamental wind statistics for the Kennedy Space Center are specified in terms of peak wind speeds for various periods of exposure (hour, day, month, etc.) at a reference height of 10 meters. A statistical peak wind profile model is used to extrapolate this information into the vertical, and the mean wind profile for various averaging periods is obtained by applying gust factors.

4.1. Peak Wind Profiles

To develop a peak wind profile model, about 6,000 hourly peak wind speed profiles measured during 1967 at the tower were analyzed. The data seemed

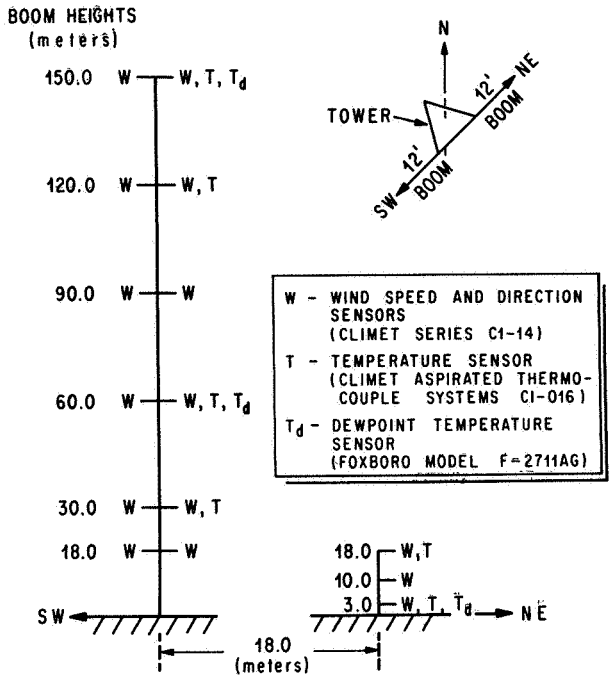

FIGURE 5. Schematic diagram of the location of instrumentation of the NASA 150-meter meteorological tower at Kennedy Space Center, Florida.

to show that the variation of the peak wind speed in the vertical, below 150 meters, could be described with a power law relationship given by

$$u(z) = u_{18}(z/18)^k, \tag{1}$$

where $u(z)$ is the peak wind speed at height z above natural grade and u_{18} is a known peak wind speed at $z = 18$ meters. The parameter k was determined for each profile by a least-squares analysis of the data.

At low wind speeds on the order of 2 m sec^{-1}, the values varied from about -0.05 to 0.15. Negative values of k occurred for approximately 8% of the cases in the sample. One should keep in mind that we are analyzing peak wind profiles and that it is possible for the peak wind speed at some or all of the levels about 18 meters to be less than the 18-meter level peak wind speed resulting in negative values of k. This is not to imply that the associated mean wind speeds decrease in the vertical.

A statistical analysis of the data revealed that, for engineering purposes, k is distributed normally for any particular value of the peak wind speed at the 18-meter level. Thus, for a given percentile level of occurrence, it was found that, for peak wind speeds at the 18-meter level less than approximately 2 m sec^{-1}, k is equal to a constant, while for peak wind speeds greater than 2 m sec^{-1},

$$k = b\, u_{18}^{-3/4}, \tag{2}$$

where b is a parameter that is distributed normally with mean value $\bar{k}$ and variance σ equal to 0.52 and 0.36 and u_{18} is in meters per second. The distribution of k as a function of u_{18} is shown in Figure 7

To apply Eqs. (1) and (2) to the peak wind statistics valid at 10 meters, Eq. (1) is evaluated at $z = 10$ m, and it is assumed that the resulting relationship can be inverted to yield u_{18} as a function of the 10-meter level peak wind speed u_{10} for a

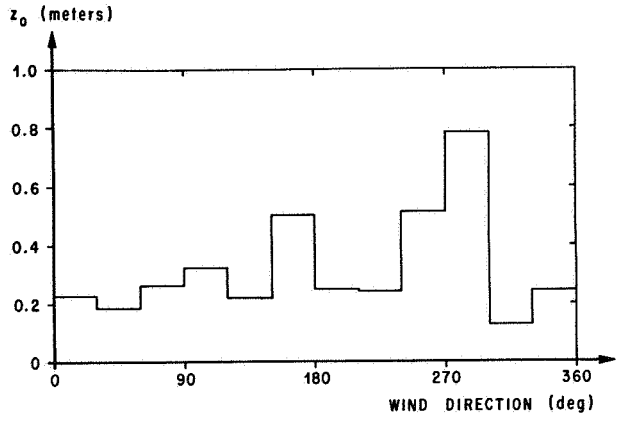

FIGURE 6. Distribution of the surface roughness length at the NASA 150-meter meteorological tower site.

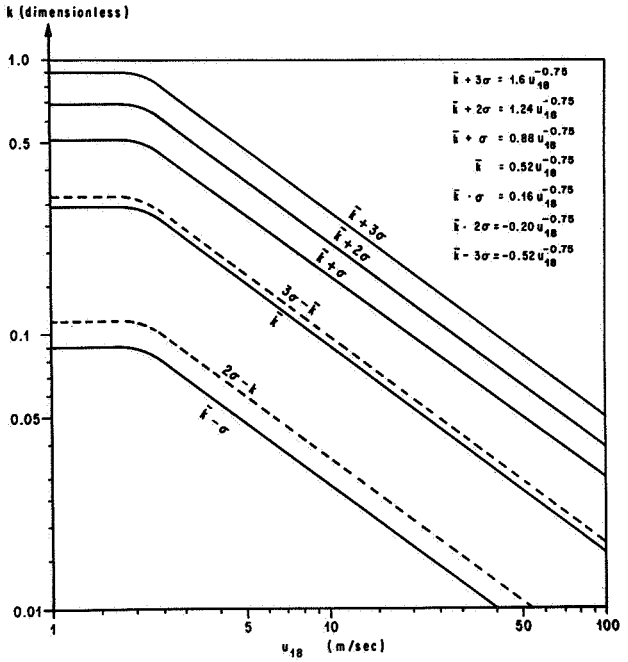

FIGURE 7 The mean, $\pm\sigma$, $\pm 2\sigma$, and $\pm 3\sigma$ values of k as functions of the peak wind speed u_{18} at the 18-meter level.

fixed value of b. This function is then combined with Eq. (2) to yield k as a function of u_{10} for a given value of b. The validity of this inversion process is open to question because Eq. (1) is a stochastic relationship. However, preliminary analyses of profiles that include peak wind information obtained at the 10-meter level seem to show that this inversion is valid.

The current design practice at MSFC is to use the $\bar{k}+3\sigma$ value of k to determine operational limits for space vehicles. Thus, if a space vehicle designed to withstand a particular value of the peak wind speed at the 10-meter level is exposed to that peak wind speed, the vehicle has at least a 99.87 percent chance of withstanding the associated peak wind speed profile.

4.2. Alternative Approach

At the present time, we are developing procedures to extrapolate peak wind speed distributions valid at the 10-meter level to other levels. Consider a peak wind speed probability density function (p.d.f.) $p_1(u_{10})$ valid at the 10-meter level for a given period of exposure, say, one hour. The probability that u_{10} is less than u_{10c} is given by

$$p(u_{10}<u_{10c}) = \int_0^{u_{10c}} p_1(u_{10})\, du_{10}. \tag{3}$$

To obtain the peak wind speed p.d.f., at level z, we express Eq. (1) in the form

$$u_{10}(u_z, b) = u_z(10/z)^{b[u_{18}(u_z,b)]-3/4}, \tag{4}$$

where we assume that Eqs. (1) and (2) can be inverted to yield u_{18} as a function of b and the peak wind at level z denoted by u_z. Eq. (4) permits us to express Eq. (3) in the form

$$p(u_z<u_{zc} \mid b) = \int_0^{u_{zc}} p_1(u_{10}(u_z, b)) \left(\frac{\partial u_{10}}{\partial u_z}\right)_b du_z, \tag{5}$$

where $p(u_z<u_{zc} \mid b)$ is the conditional probability that u_z is less than u_{zc}, given b and $p(u_z<u_{zc} \mid b) = p(u_{10}<u_{10c})$. Thus, the integrand in Eq. (5) is the conditional p.d.f. of u_z, given b, and is given by

$$p_2(u_z \mid b) = p_1(u_{10}(u_z, b)) \left(\frac{\partial u_{10}}{\partial u_z}\right)_b \tag{6}$$

The quantity $(\partial u_{10}/\partial u_z)_b$, a function of u_z and b, can be calculated by differentiating Eq. (4). The joint p.d.f. of u_z and b is given by

$$p_2(u_z, b) = p_1(u_{10}(u_z, b)) \left(\frac{\partial u_{10}}{\partial u_z}\right)_b p(b), \tag{7}$$

where $p(b)$ is the p.d.f. of b, a known function. Upon integrating Eq. (7) over the range of b, we obtain the marginal p.d.f. of u_z:

$$p_2(u_z) = \int_{-\infty}^{\infty} p_1(u_{10}(u_z, b)) \left(\frac{\partial u_{10}}{\partial u_z}\right) p(b)\, db. \tag{8}$$

At the present time, we are calculating these integrals numerically for the annual hourly peak wind speed data. To calculate the monthly and seasonal peak wind speed statistics, we require the associated monthly and seasonal distributions of k. Programs are now being written to calculate these statistics.

Once we have determined the p.d.f. of the peak wind speed as a function of height, we can then calculate design peak wind-speed profile envelopes for various percentile levels of occurrence.

4.3. Instantaneous Extreme Wind Profiles

Because the probability that the hourly peak wind speeds at all levels occur simultaneously is small, the practice of using peak wind profiles introduces some conservatism into the design criteria. This section estimates the amount of conservatism involved.

To gain some insight into this question, about 35 hours of digitized magnetic tape data were analyzed. The data were digitized at 0.1-second intervals in real time and partitioned into 0.5-, 2-, 5-, and 10-minute samples. The vertical average peak wind speed $\bar{u}_P$ and the 18-meter mean wind $\bar{u}_{18}$ were calculated for each sample. In addition, the instantaneous vertical average wind speed time history at 0.1-second intervals was calculated for each sample, and the peak instantaneous vertical average wind speed $\bar{u}_I$ was selected from each sample. The quantity $\bar{u}_I/\bar{u}_P$ was then interpreted to be a measure of how well the peak wind profile statistics at the 10-meter level approximate the instantaneous extreme wind profile statistics.

In Figure 8, a plot of $\bar{u}_I/\bar{u}_P$ as a function of $\bar{u}_{18}$, the data points tend to scatter about a mean value

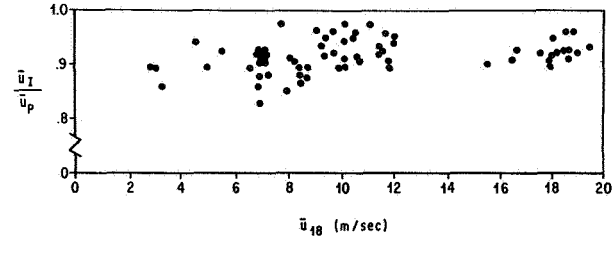

FIGURE 8. The ratio $\bar{u}_I/\bar{u}_P$ as a function of the mean wind speed $\bar{u}_{18}$ at the 18-meter level for an averaging time equal to 10 minutes.

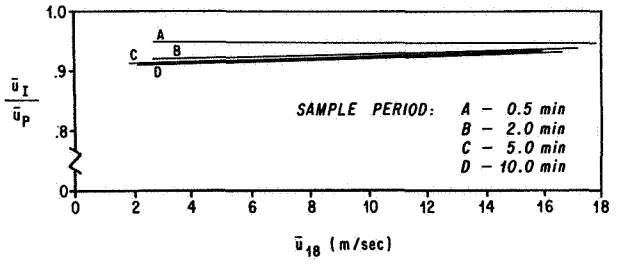

FIGURE 9 The ratio $\bar{u}_I/\bar{u}_P$ as a function of the mean wind speed $\bar{u}_{18}$ at the 18-meter level for averaging times equal to 0.5 (*A*), 2 (*B*), 5 (*C*), and 10 minutes (*D*).

of $\bar{u}_I/\bar{u}_P \simeq 0.93$. Since drag loads are proportional to the square of the velocity, this mean value implies that the peak wind profile may be overestimating the loads by about 14%. However, the fact that some of the data points have values equal to 0.98 could mean an overestimate of the loads by only 4%. Figure 9 gives the average values of $\bar{u}_I/\bar{u}_P$ as a function of $\bar{u}_{18}$ for different averaging times (0.5, 2, 5, and 10 minutes)

4.4. Gust Factor

The gust factor G is defined as

$$G = u/\bar{u}, \tag{9}$$

where u is the peak wind speed within a data record of length t in time and $\bar{u}$ is the mean wind speed associated with the data record. A simple theory can be constructed to aid in understanding the behavior of the gust factor. If σ denotes the variance of the fluctuations of velocity about the mean wind speed, then $\bar{u}+3\sigma$ is an estimate of the peak wind speed, therefore,

$$G = 1 + \frac{3\sigma}{\bar{u}} \tag{10}$$

The variance is related to the friction velocity, u_*, through the relationship

$$\sigma = A(Ri, t)\, u_*, \tag{11}$$

where A is a function of the Richardson number, Ri, and the averaging time, t. The Richardson number is given by

$$Ri = \frac{\dfrac{g}{\bar{T}}\left(\dfrac{g}{C_p} + \dfrac{d\bar{T}}{dz}\right)}{\left(\dfrac{d\bar{u}}{dz}\right)^2}, \tag{12}$$

where $\bar{T}$ and $\bar{u}$ denote the mean Kelvin temperature and wind speed at height z, g is the acceleration of gravity, and C_p is the specific heat of dry air at constant pressure ($g/C_p \simeq 9.8$°K/km). In approximately the first 30 meters of the boundary layer, the wind profile is given by

$$\bar{u} = \frac{u_*}{k_1}\left(\ln\frac{z}{z_0} - \psi(Ri)\right) \tag{13}$$

where k_1 is von Karman's constant with numerical value approximately equal to 0.4, z_0 is the surface roughness length and $\psi(Ri)$ is a universal function of Ri.

Combining Eqs. (9), (10), (11) and (13), we find that

$$G = 1 + \frac{3k_1 A(Ri, t)}{\ln\dfrac{z}{z_0} - \psi(Ri)} \tag{14}$$

For a neutral atmosphere, $Ri = 0$, and ψ vanishes, so that

$$G = 1 + \frac{3k_1 A(0, t)}{\ln\dfrac{z}{z_0}} \tag{15}$$

We may conclude from this relationship that the gust factor decreases as the height increases. This result is also qualitatively true for unstable air ($Ri < 0$). As the averaging time decreases, the variance will decrease so that A is a decreasing function of the averaging time and thus, we may conclude from (14) that G is an increasing function of the averaging time.

The functions ψ and A are monotonically decreasing functions of the Richardson number; ψ vanishes in neutral ($Ri = 0$) air, while A is positive definite. Thus, as the Richardson number decreases, or rather, as the air becomes more unstable, the gust factor increases.

Let us now consider a typical daytime situation at Cape Kennedy. At low wind speeds the air is unstable and G is large. However, as the wind speed increases, the wind shear ($d\bar{u}/dz$) increases, causing the Richardson number to tend to zero from the unstable side of $Ri = 0$. Thus, an increase in the wind speed will tend to lower the gust factor in view of the dependence of the gust factor upon stability. In a typical nighttime situation, the stratification is stable, and the Richardson number is usually positive. As the wind speed increases, the

Richardson number tends to zero from the stable side of $Ri=0$. This means that the gust factor will increase as the wind speed increases. In both cases the limiting value of the gust factor will be that of a neutral atmosphere ($Ri=0$) as given by Eq. (15).

In view of these considerations, a gust factor model for the Kennedy Space Center was developed with 181 hours of afternoon turbulence data encompassing a broad range of wind speed conditions. Gust factors were calculated for averaging times (t) equal to 0.5, 1, 2, 5, 10 and 60 minutes. It was assumed that the gust factor is a function of the averaging time t, and the peak wind speed u_{18} at the 18-meter level. The peak wind speed at the 18-meter level plays the role of a stability parameter. It was found that the expected value of the gust factor at any level between 18 and 150 meters can be represented as

$$G=1+\frac{1}{g_0}(18/z)^p, \tag{16}$$

where z is the height in meters. In this equation the parameters p and g_0 are given by

$$p=0.283-0.435e^{-0.2u_{18}} \tag{17}$$

and

$$g_0=1.98+0.085\left(\ln\frac{t}{10}\right)^2-0.329\ln\frac{t}{10}-1.887e^{-0.2u_{18}}, \tag{18}$$

where t and u_{18} have the units of minutes and meters per second. The dependence of the 18-meter level gust factor on the averaging time and the peak wind speed is shown in Figure 10, and the dependence of the 10-minute gust factor on the peak wind speed and height is given in Figure 11.

Within the range of variation of the data, the 1-hour gust factor and the 10-minute gust factor were approximately equal, because the spectrum of the horizontal wind speed near the ground is characterized by a broad energy gap centered at a frequency approximately equal to 1 cycle hr^{-1} and typically extends over the frequency domain 0.5 cycles

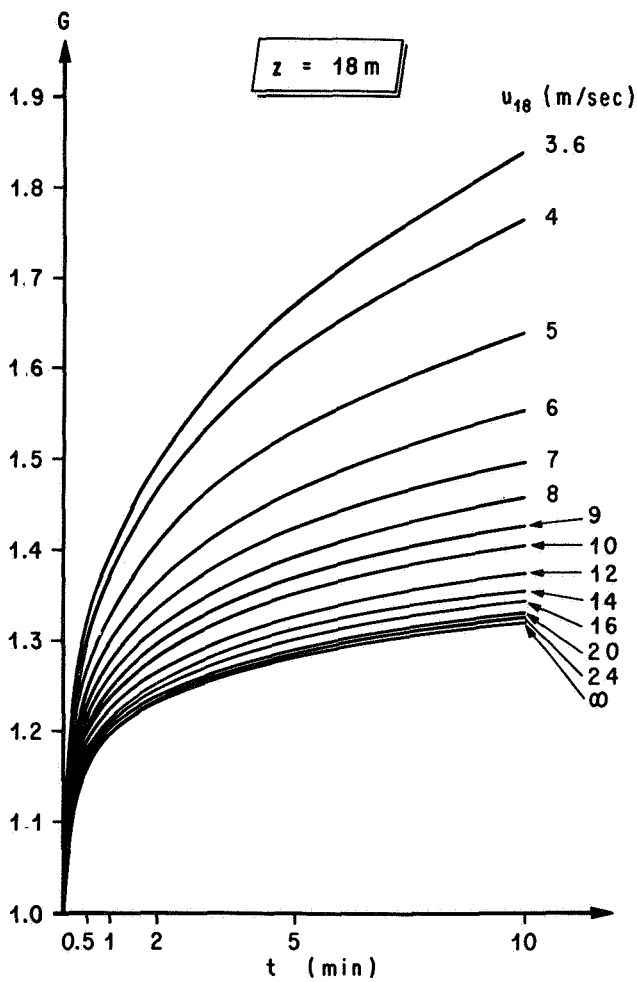

FIGURE 10. The gust factor G at the 18-meter level as a function of the averaging time for various peak wind speeds at the 18-meter level.

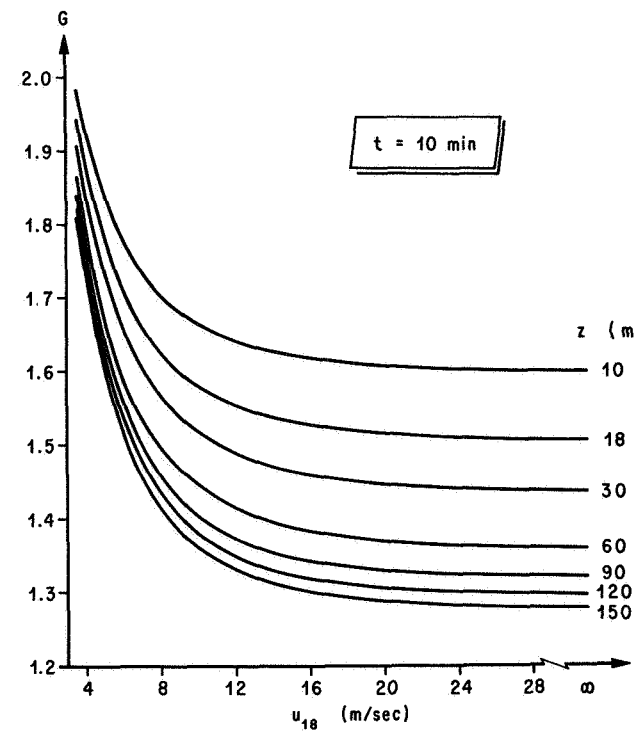

FIGURE 11 The gust factor G as a function of the peak wind u_{18} at the 18-meter level for various heights above natural grade associated with a 10-minute grand average.

$hr^{-1} < n < 5$ cycles hr^{-1} [7]. The spectral components associated with frequencies less than 1 cycle hr^{-1} correspond to the mesoscale and synoptic scale motions, while the remaining high frequency spectral components correspond to mechanically and thermally produced turbulence. Thus, a statistically stable estimate of the mean or steady-state wind speed can be obtained by averaging over a period in the range from 10 minutes to an hour. Davenport [8] points out that this period for averaging is also suitable for structure analysis. He also points out that, since this period is far longer than any natural period of structural vibration, it assures that effects caused by the mean wind properly represent steady-state, non-transient effects. At the present time, the 10-minute gust factors and the design peak wind profile are used to obtain a design mean wind profile.

5. Design Spectral Models

In many types of space vehicle response calculations, engineers have used the Fourier transform to solve the equations of motion which describe and predict the ultimate response of the space vehicle to the natural environment. Thus, the input function which describes the turbulent character of the drag loads must be specified in terms of Fourier amplitudes. Motivated by this requirement, the atmospheric scientists at the Marshall Space Flight Center, the Cornell Aeronautical Laboratories, and Pennsylvania State University have embarked upon an extensive program to define the spectral nature of the longitudinal and lateral components of turbulence at the Kennedy Space Center, Florida.

To establish a spectral model of turbulence for the Kennedy Space Center, approximately fifty cases of turbulence were analyzed. The procedure used to calculate the longitudinal and lateral components of turbulence consisted of (1) converting the digitized wind speeds and directions (10 data points per second) into the associated north–south and east–west components and averaging these components over the duration time of each test, (2) calculating the mean wind speed and direction with the averaged components, (3) projecting the original digitized data onto the mean wind vector and subtracting the mean wind speed to yield the longitudinal components of turbulence, and (4) projecting the original digitized data onto a normal-to-the-mean-wind vector to obtain the lateral components of turbulence. Trends contained within the data were removed by fitting the longitudinal and lateral components of turbulence to second order polynomials and in turn subtracting these polynomials from the component time histories. To reduce computation time, the data, with trend removed, were block-averaged over half second intervals. The longitudinal and lateral spectra were calculated by using the standard correlation Fourier transform methods given by Blackman and Tukey [9]. These spectra were corrected for the half-second block-averaging operation with the procedure given by Pasquill [10] and for the response properties of the instrumentation.

To combine the spectra for each level on the tower, it was assumed that the similarity theory of Monin [11] for the vertical velocity spectrum could be applied to the longitudinal and lateral spectra, so that

$$\frac{nS(n)}{u_*^2} = F(f, Ri), \tag{19}$$

where $nS(n)$ is the logarithmic longitudinal or lateral spectrum associated with frequency n (cps), and u_* is the surface friction velocity, or rather, the square root of the tangential eddy stresses per unit mass. F is tentatively a universal function of the dimensionless wave number f and the gradient Richardson number Ri. The dimensionless wave number is given by

$$f = \frac{nz}{\bar{u}(z)} \tag{20}$$

Since the tower does not yet have the capability to measure vertical velocity fluctuations, the Reynolds stress, and hence u_*^2, cannot be calculated with first principles, viz., $u_*^2 = \langle -u'w' \rangle$, where u' and w' are the longitudinal and vertical velocity fluctuations and the angular brackets denote a time-averaging operator. However, an estimate of the surface friction velocity can be calculated from mean wind and temperature profile data.

According to Lumley and Panofsky [7], the mean wind profile in approximately the first 30 meters of the atmosphere is given by

$$\bar{u}(z) = \frac{u_*}{k_1}\left\{\ln\frac{z}{z_0} - \psi\left(\frac{z}{L'}\right)\right\}, \tag{21}$$

where k_1 is von Karman's constant with numerical value approximately equal to 0.4, and ψ is a universal function of z/L' L' is a stability length given by

$$L' = \frac{u_* \frac{d\bar{u}}{dz} \bar{T}}{k_1 g \left(\frac{g}{C_p} + \frac{d\bar{T}}{dz} \right)}, \quad (22)$$

where $\bar{T}$ is the Kelvin temperature associated with the mean flow z/L' is related to the Richardson number Ri through the relationships

$$\frac{z}{L'} = \frac{Ri}{(1-18Ri)^{1/4}} \qquad (Ri < -0.01), \quad (23)$$

$$\frac{z}{L'} = Ri \qquad (-0.01 \leqq Ri \leqq 0.01), \quad (24)$$

and

$$\frac{z}{L'} = \frac{Ri}{1-7Ri} \qquad (0.1 \geqq Ri > 0.01) \quad (25)$$

Eq. (23) is a form of the KEYPS [7] equation. The function $\psi(z/L')$ associated with Eqs. (24) and (25) are given by

$$\psi(z/L') = -4.5 \frac{z}{L'} \qquad (-0.01 \leqq Ri \leqq 0.01) \quad (26)$$

and

$$\psi(z/L') = -7 \frac{z}{L'} \qquad (0.1 \geqq Ri > 0.01) \quad (27)$$

Lumley and Panofsky [7] have graphically indicated the function $\psi(z/L')$ for $Ri < -0.01$ and the function

$$\psi(z/L') = 0.044 \left(\frac{-z/L'}{0.01} \right)^{1.0674 - 0.678 \ln (-z/L'/0.01)} \qquad (Ri < -0.01) \quad (28)$$

faithfully reproduces their curve.

The calculation of u_* was based upon the wind data measured at the 18- and 30-meter levels and the temperature data measured at the 18- and 60-meter levels. Temperatures at the 30-meter level were estimated by logarithmically interpolating between the 18- and 60-meter levels. An estimate of the gradient Richardson number, Eq. (12), at the 23-meter level (geometric mean height between the 18- and 30-meter levels) was determined by assuming that the mean wind speed and temperature are logarithmically distributed between these levels. The gradient Richardson number estimated in this manner is given by

$$Ri(z_g) = \frac{g}{\bar{T}(z_g)} \left\{ \frac{\bar{T}(z_2) - \bar{T}(z_1)}{z_g \ln (z_2/z_1)} + \frac{g}{C_p} \right\} \times \left\{ \frac{\bar{u}(z_2) - \bar{u}(z_1)}{z_g \ln (z_2/z_1)} \right\}^{-2}, \quad (29)$$

where $\bar{T}(z)$ is the mean temperature at height z, z_1, and z_2 denote 18 and 30 meters, $z_g = \sqrt{z_1 z_2}$.

To calculate u_*, z_g/L' was evaluated for each case by means of one of the three Eqs. (23) through (25) corresponding to the appropriate Richardson number. L' was then assumed to be invariant with height, and $\psi(18/L')$ was estimated with Eqs. (26) through (28). Eq. (21) was then evaluated at the 18-meter level and solved to yield u_*. The values of z_0 used for this calculation are given in Section IIIc.

The meteorological conditions of particular interest are those associated with mean wind speeds at the 18-meter level greater than approximately 10 m sec^{-1}. During these flow conditions, the boundary layer is well mixed so that vertical gradients of the mean flow entropy are small ($d\bar{T}/dz \simeq -g/C_p$) and the wind shears are large; thus, the Richardson number vanishes or at least becomes very small. Accordingly, the neutral longitudinal and lateral spectra are of particular interest in the design and operation of space vehicles. The neutral spectra were determined by extrapolating the data to $Ri = 0$ by the procedure developed by Berman [12]. Scaled spectra $nS(n)/u_*^2$ were plotted against Ri for various values of f, and curves were drawn by eye. Of course, the data points scattered about this line. The values of $nS(n)/u_*^2$ at $Ri = 0$ were then read off to yield the neutral spectra for the various levels on the tower. The results of this graphical process are shown in Figures 12 and 13.

In Figures 12 and 13 the position of the maxima shift toward higher values of f as the height increases. This means that Monin coordinates $(nS(n)/u_*^2, f)$ fail to collapse the spectra in the vertical so that $F(f, Ri)$ is not a universal function, and thus an added height dependence should be included in the analysis. Busch and Panofsky [13] have obtained similar results from analyses of tower data from Round Hill. The failure of the Monin coordinates to collapse the spectra in the vertical can be attributed to vertical variations in both the Reynolds stress and the length scale used to scale the wave number $n/\bar{u}(z)$

Above the Monin layer ($z < 30m$) in the Ekman layer ($z > 30m$), the tangential Reynolds stress decreases with height. In addition, the variances of

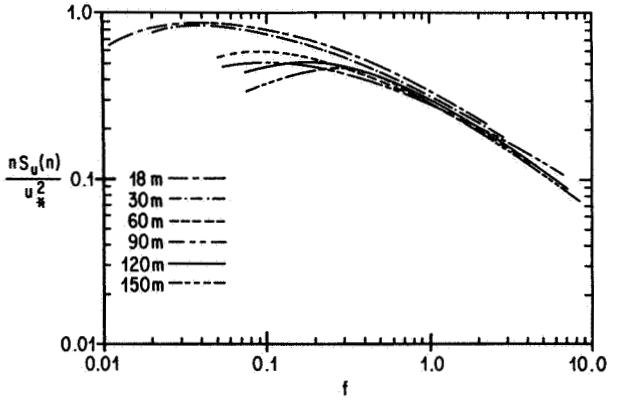

FIGURE 12. Dimensionless logarithmic longitudinal spectra for neutral wind conditions plotted in Monin coordinates.

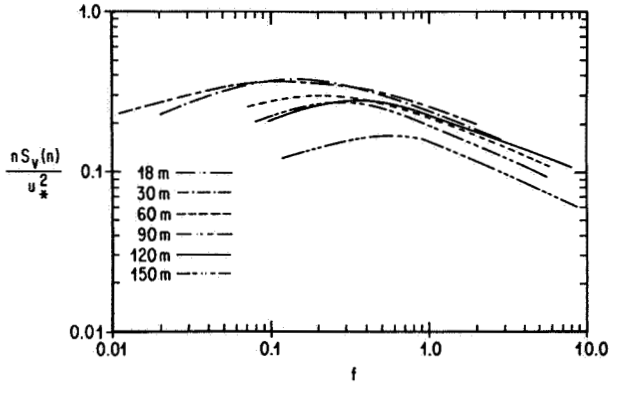

FIGURE 13. Dimensionless logarithmic lateral spectra for neutral wind conditions plotted in Monin coordinates.

the longitudinal and lateral components of turbulence are decreasing functions of z, so that by scaling the spectra with the surface value of the friction velocity, the scaled spectra at the upper levels fall below the 18-meter spectra.

By scaling the wave number with z, we have assumed that the integral scales of the longitudinal and lateral components of turbulence are proportional to z. This might be true in the Monin layer, however, in the Ekman layer one might suspect from the behavior of eddy coefficients [14] that, if the local integral scales have a vertical variation, then they should increase at a rate slower than z. In addition, we have no knowledge that the integral scales of the longitudinal and lateral spectra should have the same vertical variation. However, the data appear to show that Monin coordinates will collapse spectra with various turbulence intensities at any particular level in the vertical.

To produce a vertical collapse of the data, it was assumed, for engineering purposes, that the spectra in Monin coordinates are shape-invariant in the vertical. This hypothesis appears to be reasonable and permits a practical approach to developing an engineering spectral model of turbulence.

5.1. The Longitudinal Spectrum

The vertical variation of the dimensionless wave number f_{mu} associated with the peak of the logarithmic spectrum S_u scaled in Monin coordinates is given in Figure 14. A least-squares analysis of the data in this figure yields the result

$$f_{mu}=0.03(z/18), \tag{30}$$

where z is in meters. A plot of $nS_u(n)/u_*^2$ versus f/f_{mu} will shift the spectra at the various levels, so that all the peaks of the logarithmic longitudinal spectra are located at $f/f_{mu}=1$ Values of f_{mu} from other tower sites are indicated in Figure 14.

The average ratio β_u of the shifted spectrum at level z and the 18-meter spectrum,

$$\left(S_u(f/f_{mu}, z)/S_u(f/f_{mu}, 18)\right),$$

is shown in Figure 15. A least-squares analysis of these data yielded the result

$$\beta_u=(z/18)^{-0.63}, \tag{31}$$

where z is in meters. A plot of $nS_u(n)/\beta_u u_*^2$ versus f/f_{mu} will collapse the longitudinal spectra. The collapsed longitudinal data are plotted as a function

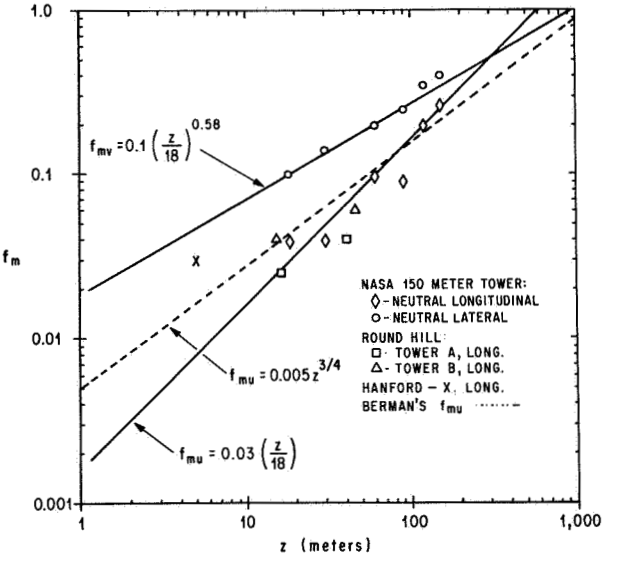

FIGURE 14. Vertical distributions of the dimensionless frequencies f_{mu} and f_{mv} associated with the peak of the logarithmic longitudinal and lateral spectra for neutral stability conditions.

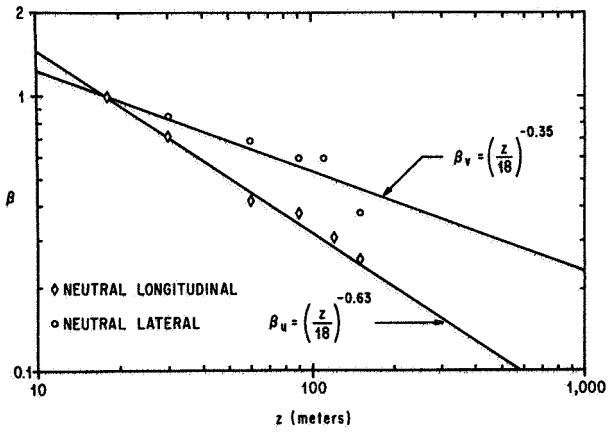

FIGURE 15. The vertical distribution of the collapsing factors β_u and β_v for neutral stability conditions.

of $0.03f/f_{mu}$ in Figure 16.

The function

$$\frac{nS_u(n)}{\beta_u u_*^2} = \frac{C_u f/f_{mu}}{(1+1.5(f/f_{mu})^{r_u})^{5/3r_u}} \tag{32}$$

was selected to represent the longitudinal spectrum, where C_u and r_u are positive constants, determined by a least-squares analysis. For sufficiently small values of f, $nS_u(n)/\beta_u u_*^2$ asymptotically behaves like f/f_{mu} which is the correct behavior for a one-dimensional spectrum. At large values of f, $nS_u(n)/\beta_u u_*^2$ asymptotically behaves like

$$(f/f_{mu})^{-2/3},$$

consistent with the concept of the inertial subrange. The maximum value of (32) occurs at $f=f_{mu}$. Various authors have suggested formulae like (32) to represent the longitudinal spectrum. However, most of the representations have only one adjustable parameter available, while Eq. (32) has two: C_u and r_u. In this light (32) appears to be superior. Upon setting $r_u=5/3$, we obtain the form of the longitudinal spectrum suggested by Panofsky [7] to represent the strong wind spectra of Davenport [15]. Von Karman's longitudinal spectrum [16] can be obtained by setting $r_u=2$. A least squares analysis of the longitudinal data in Figure 16 revealed that $C_u=8.641$ and $r_u=0.845$.

5.2. The Lateral Spectrum

The lateral spectra S_v can be collapsed with a procedure like the one used for the longitudinal spectra. However, to determine an analytical expression for the lateral spectrum, special attention must be paid to the inertial subrange to guarantee that $S_u/S_v=3/4$ [17]. This requirement can be derived from the mass continuity equation for incompressible flow subject to the condition that the eddies are isotropic in the inertial subrange. The experimental values of f_{mv} and β_v are given in Figures 14 and 15. These data show that f_{mv} and β_v can be represented as power laws as for the longitudinal spectra. The function

$$\frac{nS_v(n)}{\beta_v u_*^2} = \frac{C_v f/f_{mv}}{(1+1.5(f/f_{mv})^{r_v})^{5/3r_v}} \tag{33}$$

was used to represent the scaled spectra, where C_v and r_v are positive constants. This function behaves like the one chosen for the longitudinal spectrum.

For sufficiently large values of f, the asymptotic behavior of the ratio between Eqs. (32) and (33) is given by

$$\frac{S_u}{S_v} \sim \frac{C_u}{C_v}\frac{\beta_u}{\beta_v}\left(\frac{f_{mu}}{f_{mv}}\right)^{2/3}(3/2)^{5/3(1/r_v-1/r_u)} \tag{34}$$

In the inertial subrange we must have $S_u/S_v=3/4$, so that upon substituting this ratio into (34) we obtain a relationship that can be used as a constraint in the determination of values of C_v and r_v and functions to represent β_v and f_{mv}. The values $C_v=8.686$ and $r_v=0.512$, and the functions

$$f_{mv}=0.1(z/18)^{0.58} \tag{35}$$

and

$$\beta_v=(z/18)^{-0.35} \tag{36}$$

along with the longitudinal parameters will satisfy condition (34) and simultaneously give a good fit to the data (z is in meters). The collapsed lateral spectra and the functions given by (32) and (33) are shown in Figure 16.

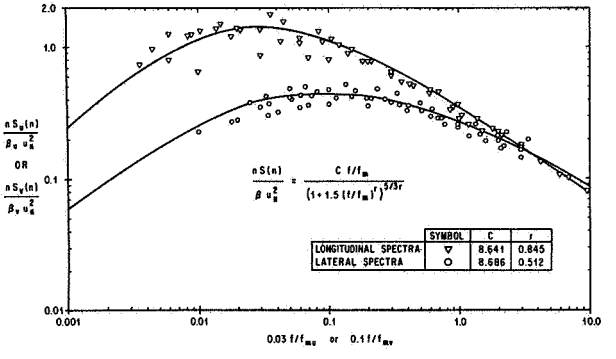

FIGURE 16. Dimensionless logarithmic longitudinal and lateral spectra as functions of $0.03\ f/f_{mu}$ and $0.1\ f/f_{mv}$ for neutral stability conditions.

5.3. Engineering Application

To apply the spectrum of turbulence to engineering problems, we first select the design peak wind speed for a prescribed level of risk. The peak wind speed profile is established by selecting the 99.87 percentile (mean $+3\sigma$) value of k, and the mean wind profile is obtained by "backing off" from the peak wind profile with the appropriate gust factor profile. The friction velocity u_* is calculated with Eq. (21) for neutral wind conditions ($Ri=0$, $\psi(0)=0$). Once the mean wind speed profile and the friction velocity are known, the longitudinal and lateral spectra are completely specified. This is the procedure presently used at MSFC.

Thus far, we have been talking about the spectra of the longitudinal and lateral components of turbulence. Actually, it is the spectra of the square of these components that are important from a loads viewpoint. If we assume that these components individually constitute Gaussian processes, then it is possible to express the power spectra of $(\bar{u}+u')^2$ or v'^2 with the Wiener-Khintchine theorem in the form

$$S_2(n)=[(\bar{u}^4+2\bar{u}^2\sigma^2)\epsilon+\sigma^4]\delta(n)+4\epsilon\bar{u}^2S_1(n)+2\int_{-\infty}^{\infty}S_1(n-\xi)S_1(\xi)\,d\xi, \quad (37)$$

where $S_2(n)$ is defined in the interval $-\infty<n<\infty$, $\epsilon=1$ (longitudinal loads) or 0 (lateral loads) and $\delta(n)$ is the Dirac delta function. In this equation, the variance of the turbulence is given by

$$\sigma^2=\int_0^{\infty}S(n)\,dn, \quad (38)$$

where $S(n)$ is the longitudinal or lateral spectrum as defined by Eqs. (32) and (33) and

$$S_1(n)=\frac{S(|n|)}{2} \quad (39)$$

The details of the derivation of Eq. (37) can be found in a paper by Wood and Berry [18].

To produce the convolution integral in Eq. (37) by numerical procedures is straightforward. The right-hand side of Eq. (37) is directly proportional to the spectrum of the longitudinal or lateral drag forces, which are the required inputs for vehicle response studies.

6. Conclusions

Development of space vehicle wind loads design criteria is not simple, but is a rather complicated procedure requiring the designer and the atmospheric scientist to work as a team. The engineer must specify the risks he is willing to accept, while the atmospheric scientist must produce a wind model from which it is possible to determine the appropriate forcing functions for that accepted risk. The model presented here for Cape Kennedy, Florida, serves this purpose in that risk values can be applied to the occurrence of peak wind speeds at a reference level for a given period of exposure, and if these design peak wind speeds occur, an upper bound risk value of structural failure can be estimated from statistical information about the wind profile shape (k). By applying gust factors for an appropriate averaging period, a peak wind speed environment can be partitioned into mean wind and turbulence environments.

7. References

[1] Smith, O. E., L. W Falls, and S. C. Brown, "A Statistical Analysis of Winds for Aerospace Vehicle Design, Mission Planning, and Operations," Research Achievements Review, Vol. II, Report No. 10, Terrestrial and Space Environment at MSFC, NASA TM X-53706, George C. Marshall Space Flight Center, Huntsville, Alabama, 1967

[2] Fisher, R. A., *Contributions to Mathematical Statistics*, John Wiley and Sons, Inc., New York, 1950.

[3] Gumbel, E. J., *Statistics of Extremes*, Columbia University Press, New York, 1958,

[4] Thom, H. C. S., "Distribution of Extreme Winds in the United States," *Journal of the Structural Division, Proceedings of the American Society of Civil Engineers*, April 1960.

[5] Kaufman, J. W and L. F Keene, "NASA's 150-Meter Meteorological Tower Located at Cape Kennedy Florida " NASA TM X-53259, George C. Marshall Space Flight Center, Huntsville, Alabama, May 12, 1965.

[6] Fichtl, G. H., "An Analysis of the Roughness Length Associated with the NASA 150-Meter Meteorological Tower," NASA TM X-53690, George C. Marshall Space Flight Center, Huntsville, Alabama, January 3, 1968.

[7] Lumley, J. L. and H. A. Panofsky, *The Structure of Atmospheric Turbulence*, John Wiley and Sons, 1964.

[8] Davenport, A. G., "The Relationship of Wind Structure to Wind Loading," presented at the Meeting on Ground Wind Load Problems in Relation to Launch Vehicles, NASA Langley Research Center, June 7-8, 1966.

[9] Blackman, R. B. and J. W Tukey, *The Measurement of Power Spectra*, Dover, New York, 1958.

[10] Pasquill, F., *Atmospheric Diffusion*, D. van Nostrand Company, Ltd., New York, 1962.

[11] Monin, A. S., "On the Similarity of Turbulence in the Presence of a Mean Vertical Temperature Gradient," J. Geophys. Res., Vol. 64, 1959, pp. 2196-2197

[12] Berman, S., "Estimating the Longitudinal Wind Spectrum Near the Ground," *Quart. J Roy. Meteor Soc.*, 91, 1965, pp. 302-317

[13] Busch, N. E. and H. A. Panofsky, "Recent Spectra of Atmospheric Turbulence," *Quart. J Roy. Meteor. Soc.*, 94, 1968, pp. 132-148.

[14] Blackadar, A K et al., "Flux of Heat and Momentum in the Planetary Boundary Layer of the Atmosphere," The Pennsylvania State University Mineral Industries Experiment Station, Dept. of Meteorology, Rept under AFCRL Contract No. AF9604–6641, 1965.

[15] Davenport, A. G., "The Spectrum of Horizontal Gustiness Near the Ground in High Winds," *Quart. J Roy. Meteor Soc.*, Vol. 87, 1961, pp. 194–211.

[16] Pritchard, F E., C. G. Casterbrook, and G E. McVehil, "Spectral and Exceedance Probability Models of Atmospheric Turbulence for Use in Aircraft Design," TR AFFDL–TR–65–122, Air Force Flight Dynamics Laboratory, Research and Technology Division, Air Force Systems Command, Wright-Patterson AFB, Ohio, 1965.

[17] Batchelor, G. K., *The Theory of Homogeneous Turbulence*, Cambridge University Press, New York, 1953.

[18] Wood, J. D. and J G. Berry, "Random Excitation of Missiles Due to Winds," Proc. of National Symposium on Winds for Aerospace Vehicle Design, Vol. 1, USAF Geophysics Res. Dir A.F Surveys in Geophysics, No. 140, Vol. 1, AFCRL–62–273(I), March 1962, pp. 125–138.